BJR

Received: 22 April 2016 | Revised: 23 August 2016 | Accepted: 20 October 2016

https://doi.org/10.1259/bjr.20160362

Cite this article as:
Weisstanner C, Gruber GM, Brugger PC, Mitter C, Diogo MC, Kasprian G, et al. Fetal MRI at 3T—ready for routine use? *Br J Radiol* 2017; **90**: 20160362.

REVIEW ARTICLE

Fetal MRI at 3T—ready for routine use?

[1,2]CHRISTIAN WEISSTANNER, MD, [3]GERLINDE M GRUBER, MD, [3]PETER C BRUGGER, MD, [1]CHRISTAN MITTER, MD, [4]MARIANA C DIOGO, MD, [1]GREGOR KASPRIAN, MD and [1]DANIELA PRAYER, MD

[1]Division of Neuro- and Musculoskeletal Radiology, Department of Radiology, Medical University of Vienna, Vienna, Austria
[2]Institute for Diagnostic and Interventional Neuroradiology, Inselspital, University of Bern, Bern, Switzerland
[3]Center of Anatomy and Cell Biology, Medical University of Vienna, Vienna, Austria
[4]Neuroradiology Department, Centro Hospitalar de Lisboa Central, Lisbon, Portugal

Address correspondence to: Univ.-Prof. Dr Daniela Prayer
E-mail: *daniela.prayer@meduniwien.ac.at*

ABSTRACT

Fetal MR now plays an important role in the clinical work-up of pregnant females. It is performed mainly at 1.5 T. However, the desire to obtain a more precise fetal depiction or the fact that some institutions have access only to a 3.0 T scanner has resulted in a growing interest in performing fetal MR at 3.0 T. The aim of this article was to provide a reference for the use of 3.0 T MRI as a prenatal diagnostic method.

INTRODUCTION

Although fetal MRI was first described 1983,[1] only with recent advances in MR technologies, including the development of fast sequences introduced in the 1990s, could fetal MR be performed without sedation. In the past decade, further improvements in MR techniques led to a broader acceptance in clinical practice and the use of fetal MR as a supplementary method for the evaluation of suspicious fetal anatomy. Fetal MRI now plays an important role in the clinical work-up of pregnant females. Currently, fetal MRI is performed mainly at 1.5 T, but, recently, a growing interest in 3.0 T examinations has emerged, not only for university and research use.[2–4] The wish to perform fetal MR at 3.0 T is due to the increased signal-to-noise ratio (SNR) and probable decreased acquisition time, increased spatial resolution and ultimately a more precise fetal depiction.[5,6] Another point is that some institutions may have access only to a 3.0 T scanner. However, using fetal MRI at 3.0 T at the clinical level is challenging and there is little experience with this technique.

This review article specifically concentrates on the clinical use of fetal MR at 3.0 T and attempts to assess the advantages over 1.5 T. A systematic literature review of the most recent publications relevant to fetal MR at 3.0 T was conducted.

The aim of this article was to provide a reference for the use of 3.0 T MRI as a prenatal diagnostic method.

GENERAL ASPECTS

In general, the switch from 1.5 to 3.0 T requires an optimization of sequence parameters to maintain the desired image contrast.[7] Achieving T_1 contrast can be challenging. T_1 relaxation times (TRs) differ between the respective tissues, but are generally longer than those on 1.5 T.[7] The decreased T_1 tissue contrast on 3.0-T images may be compensated by a longer TR, which increases the duration of the sequence or parallel imaging, leading to a decrease in SNR.[8] Another possibility to increase T_1 contrast at 3.0 T is optimizing the flip angle. Ultrafast spoiled gradient-echo sequences can be used without a significant gain in time compared with 1.5 T, allowing these sequences to be performed during breath-holding. T_2 TR slightly decreases with increasing magnetic field strengths.[9] Owing to more pronounced local magnetic field inhomogeneities, T_2 decay is shorter at 3.0 T. As a result, T_2 contrast is improved but also gives rise to unwanted artefacts, which, in another point of view, increases diagnostic sensitivity, depending on the pulse sequence.[8] The SNR at 3.0 T is nearly two times as high compared with 1.5 T.[5–7] As a consequence, noise and random granular image appearance is reduced. The increased SNR can be used to improve image quality, invested into increased spatial and/or temporal resolution of dynamic sequences.

An important point at 3.0 T is artefacts. Inhomogeneities of the magnetic field are induced by the tissue interfaces, which lead to field distortion as a consequence of their susceptibility, shape and orientation relative to the field.[10] With respect to fetal MRI, this means that shimming may

Figure 1. (a) Steady-state free-precession images at 3.0 T of a fetus at 29 + 2 GW and (b) of a fetus at 31 + 5 GW at 1.5 T (Gyroscan; Philips, Best, Netherlands) with standing wave artefacts (arrows).

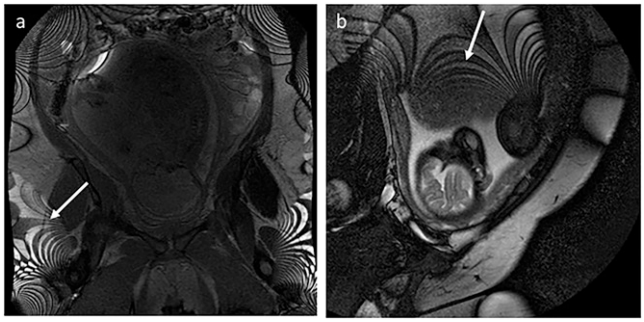

become necessary during the examination, thus increasing the overall examination time. Standing wave artefacts (Figure 1) and conductivity artefacts are two effects that are particularly strong artefacts at the end stage of pregnancy or in females with multiple pregnancies. Standing wave artefacts[11] represent regional brightening and signal loss, caused by constructive and destructive interference of the standing waves. This is because at 3.0 T, the wavelength of the radiofrequency (RF) field is on the same scale as the size of the field of view used in many abdominal MRI examinations and tends to be more pronounced with increasing field of view, such as that required in fetal MRI.[12] A related artefact, called a conductivity artefact,[13] is caused by the interaction of the RF field and highly conductive tissue or liquids in the body. As it is difficult to tackle field inhomogeneities and standing wave artefacts, a promising and more advanced technique for compensation includes multichannel transmission body coils[14,15] and several manufacturer-implemented software for reducing standing wave artefacts at 3.0 T, "MultiTransmit" (Philips, Best, Netherlands), "ZOOMit" (Siemens). In our experience, which is in line with Victoria et al,[6] steady-state free-precession (SSFP) sequences are more vulnerable to banding artefacts (Figure 2), which are off-resonance effects.[16] One way to reduce these artefacts is to optimize shimming or to adjust TR. Susceptibility artefacts deteriorate with increasing magnetic strengths (Figure 3) and can be twice as large at 3.0 T compared with that at 1.5 T.[17] Especially sensitive to these artefacts are echoplanar imaging (EPI) sequences, and this increased susceptibility brings advantage in the detection of intracranial bleed. To minimize susceptibility artefacts, readout direction can be changed, parallel imaging implemented and echo times shortened. Two other possible modifications but which lead to an SNR ratio are a wider readout bandwidth or use of smaller voxel sizes. Chemical shift artefacts are more prominent at 3.0 T than they are at 1.5 T, but owing to the fact that fetal fat is not present until later in pregnancy, it is not a significant problem in fetal imaging.[3]

Figure 2. An axial steady-state free-precession image at 3.0 T of twins at 31 + 3 GW with banding artefacts (arrows).

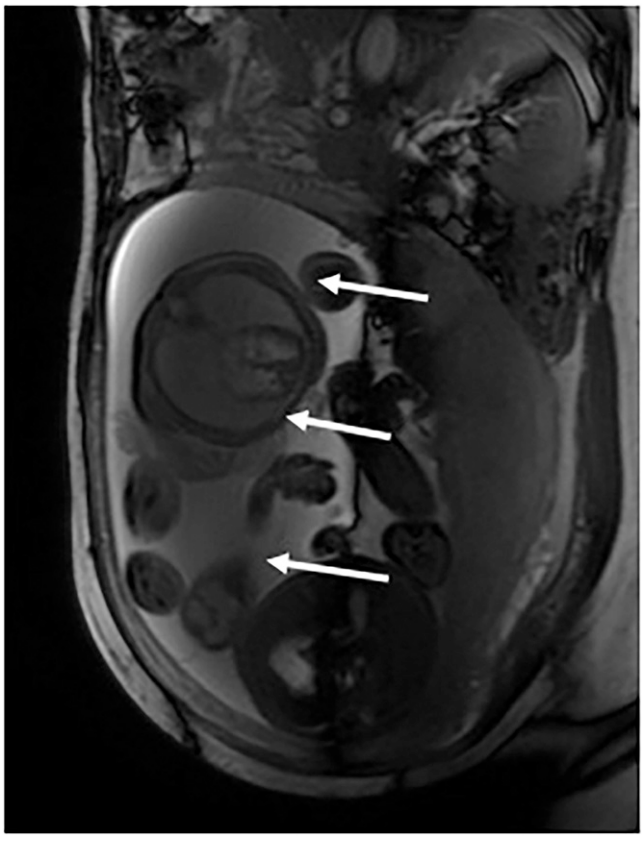

INDICATIONS

In general, indications do not differ from those at 1.5 T.[18–27]

However, regarding specific clinical questions, 3.0-T fetal MRI has the potential to supply more detailed information than lower field strengths.

Figure 3. A coronal echoplanar image of a fetus at 28 + 6 GW at 3.0 T with geometric distortion and standing wave artefacts (arrow).

Figure 4. (a) Sagittal (i), coronal (ii) and axial (iii) T_2 weighted (T2W) images and sagittal (iv), coronal (v) and axial (vi) echoplanar images at 3.0 T of a fetus at 31 + 3 GW with haemorrhage into the caudothalamic ridge (arrows). (b) Sagittal (i), coronal (ii) and axial (iii) T2W images and sagittal (iv), coronal (v) and axial (vi) echoplanar images at 1.5 T of a fetus at 33 + 0 GW with hydrocephalus and subdural haemorrhage (arrows).

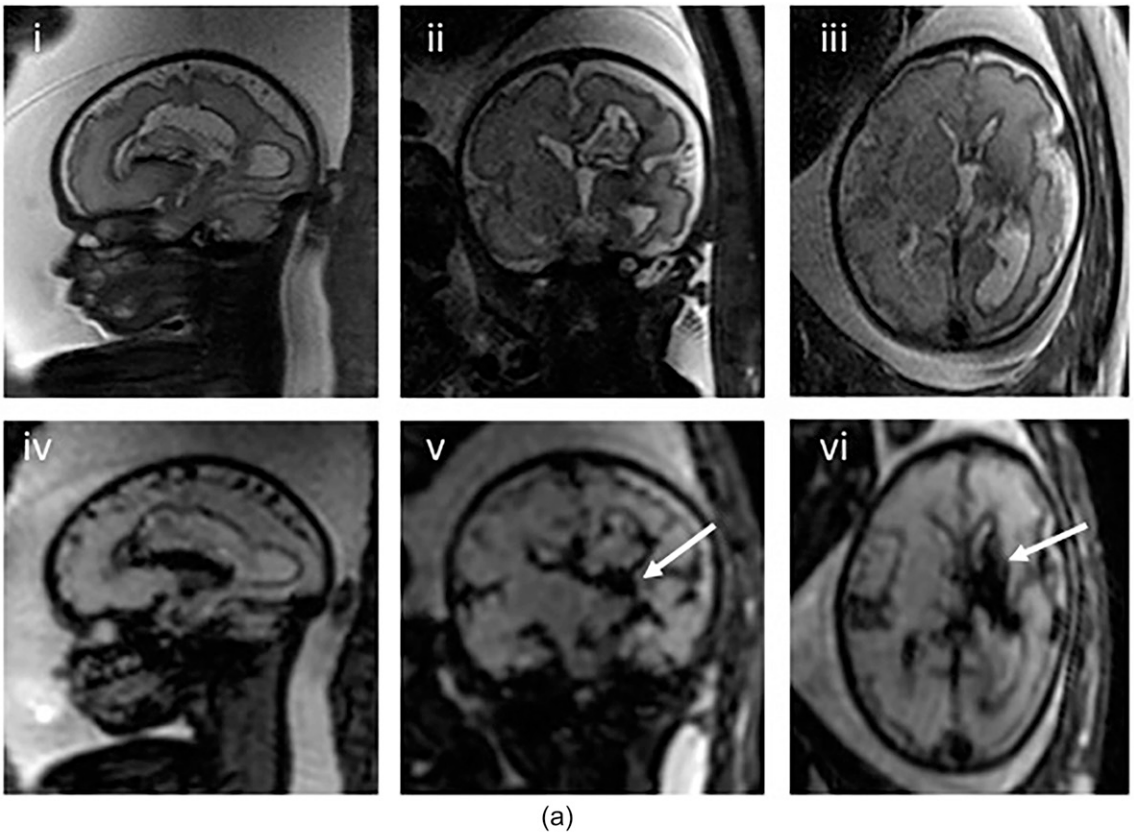

(a)

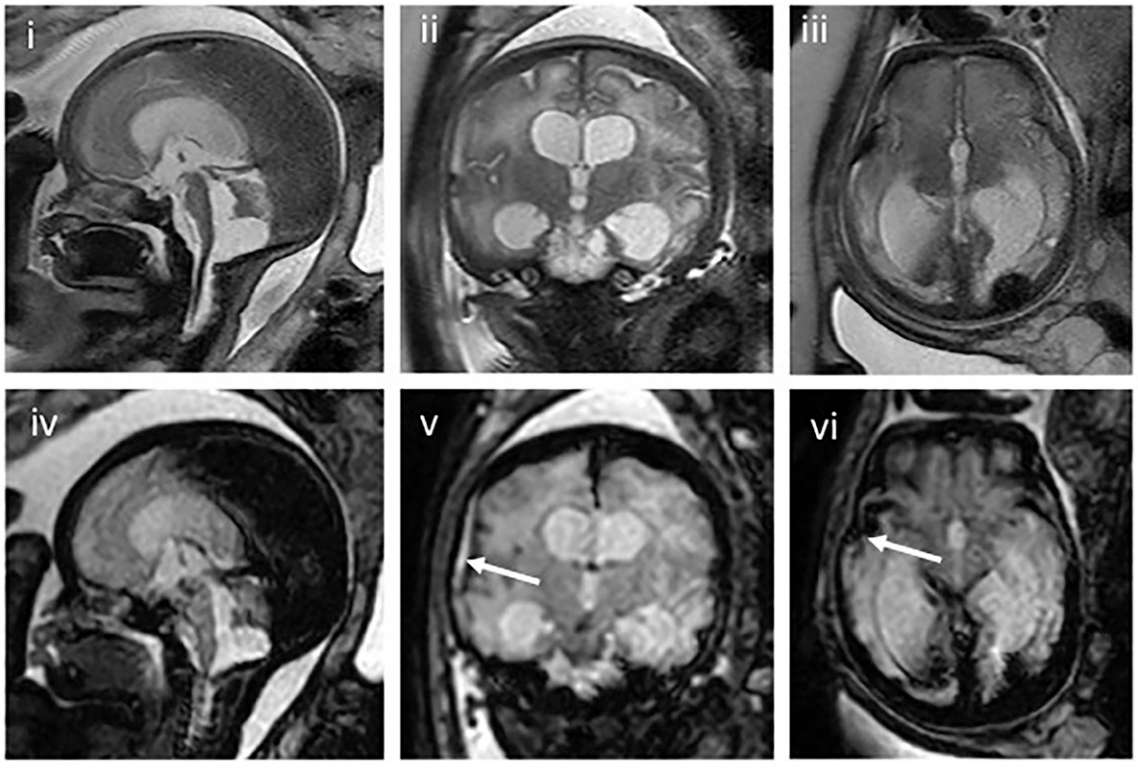

(b)

Figure 5. Sagittal (a, d) and coronal (b, c) steady-state free-precession images at 3.0 T of a fetus at 34 + 6 GW: the osseus structures and cartilage can be nicely evaluated.

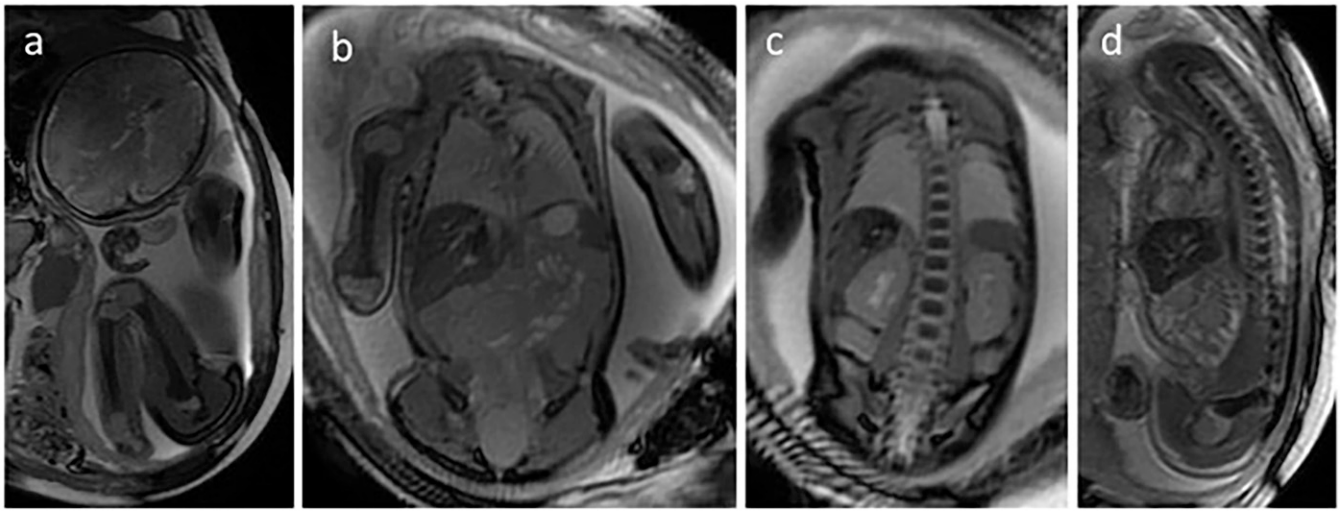

(1) The increased susceptibility at 3.0 T enhances the sensitivity for deoxyhaemoglobin, haemosiderin (Figure 4) and calcifications. In addition, bony structures are more sharply delineated even on T_2 weighted (T2W) and SSFP sequences (Figure 5).

(2) Sequences that benefit from the increased SNR at 3.0 T are T_1 weighted (T1W) and T2W sequences, diffusion tensor sequences and spectroscopy.[8] The twofold increased chemical shift effect of 3.0 T compared with 1.5 T has a positive

Figure 6. Sagittal (a), coronal (b) and axial (c) T_2 weighted (T2W) images at 3.0 T of a fetus at 19 + 2 GW with polymicrogyria. Sagittal (d), coronal (e) and axial (f) T2W images at 1.5 T of a fetus at 30 + 0 GW with polymicrogyria.

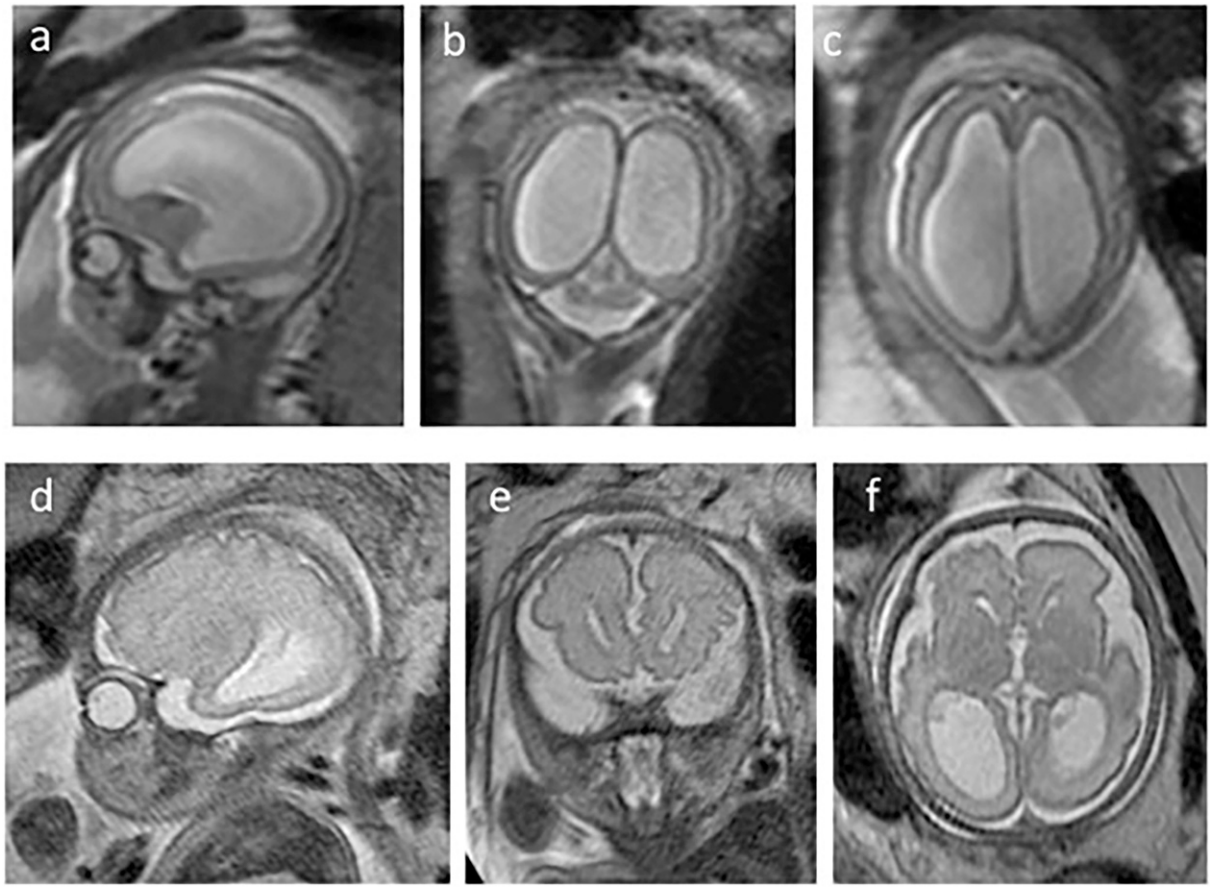

Figure 7. (a) Coronal T_2 weighted images at 3.0 T of a fetus at 21 + 4 GW and (b) at 1.5 T of a fetus at 23 + 3 GW: the ventricular/subventricular zone (short dashed arrow), intermediate zone (short arrow), subplate (long arrow) and cortical plate (long dashed arrow) can be seen.

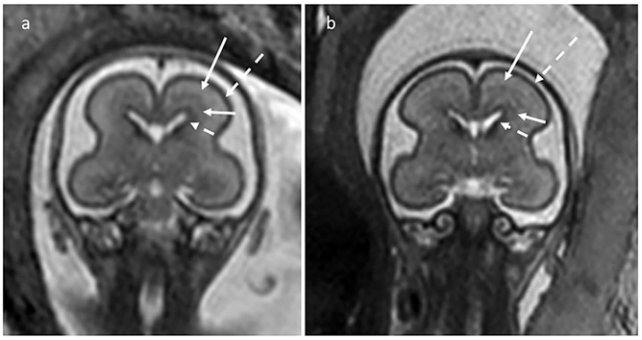

Figure 8. (a) Axial T_2 weighted images at 3.0 T of a fetus at 16 GW and (b) at 1.5 T of a fetus at 15 + 4 GW: the ventricular zone (short dashed arrow), ganglionic eminence (short arrow), subplate (long arrow) and cortical plate (long dashed arrow) can be discerned.

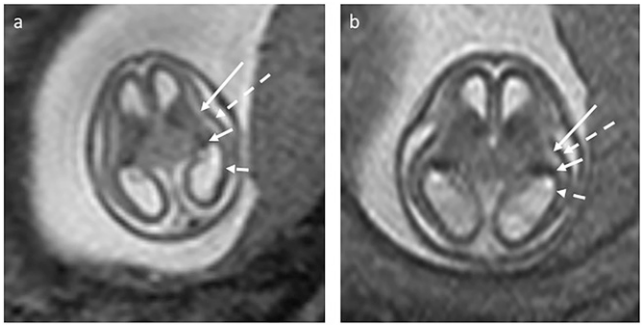

effect on the quality of spectroscopy[8] and blood oxygen level-dependent techniques.[2] These facts have an impact on especially brain imaging.

In the following, only those indications are addressed where the use of 3.0 T might be more helpful than 1.5 T.

Brain malformation

Disorders of cortical development are a common cause of neurodevelopmental delay and epilepsy. These may be very subtle and difficult to detect with ultrasound imaging. Fetal MR can depict the cerebral cortex nicely, outline abnormalities and improve the prenatal diagnosis of malformations of cortical development (Figure 6). Here, T2W sequences of good quality are very important to adequately evaluate the structure of the brain. At 3.0 T, acquisition of T2W sequences with an average slice thickness of 2–3 mm is possible, compared with 3–5 mm at 1.5 T, isovoxel (1-mm slice thickness). In addition to describing gyration and cortical sulcation, white matter development can be described by discerning the different layers of the developing brain, *e.g.* the ventricular/periventricular zone, intermediate zone, subplate and cortical plate[28] (Figure 7), and at an earlier gestational age (Figure 8).

Diffusion tensor imaging

Diffusion tensor imaging (DTI) provides better visualization of tracts. In partial or incomplete commissural agenesis, DTI helps to differentiate which commissure is absent and what kind of fibres connect the hemispheres or in cases of a tumour, how the tracts are displaced or even absent (Figure 9). The commissures are composed of the corpus callosum and the anterior and hippocampal commissure. Agenesis of the corpus callosum can be complete or partial. In complete agenesis, there are no fibres crossing the midline, and this is often associated with interhemispheric cysts and lipomas. A perfect mid-sagittal T2W slice is important to delineate the commissures (Figure 10). At 3.0 T, DTI can be acquired with a higher SNR for fibre tracking, although it is difficult to obtain high-quality images owing to the long acquisition time required[29] and movement artefacts.

Haemorrhagic lesions

In acquired brain damage, for example, the previously normally formed tissue is destroyed. There are numerous causes for this and the study of organs besides the central nervous system is important for diagnosis.[30] With the different sequences available (T2W, SSFP, fluid-attenuated inversion recovery, EPI and

Figure 9. Diffusion tensor imaging-based tractography at 3.0 T of a fetus at 33 GW with an extra-axial tumour with compression of the right hemisphere and displacement of the right corticospinal tract (yellow) to the left side. The normal-appearing left corticospinal tract is shown in green.

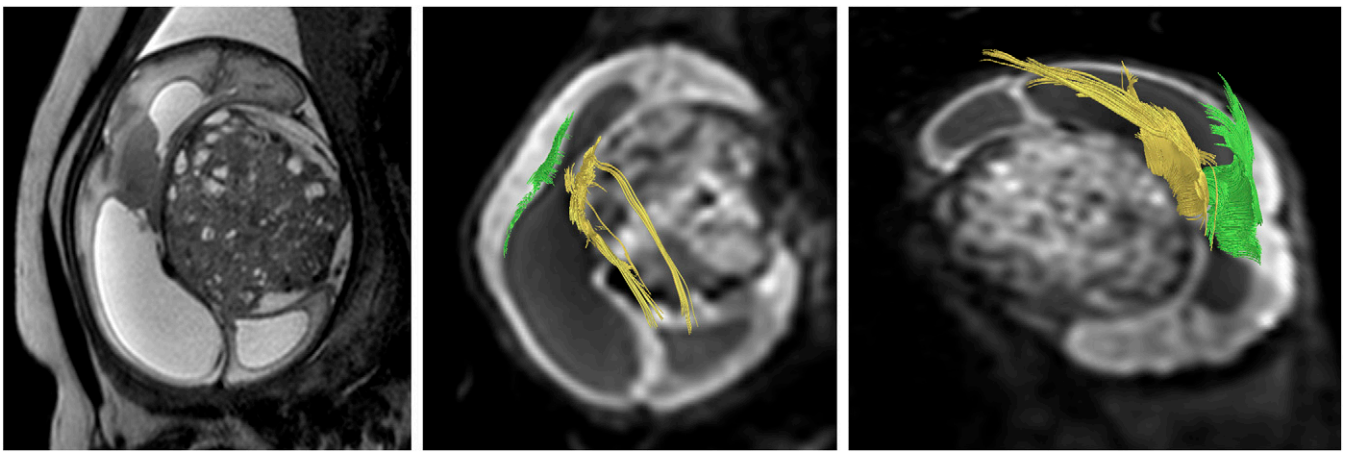

Figure 10. (a) Mid-sagittal T_2 weighted images at 3.0 T of a fetus at 23 + 3 GW and (b) at 1.5 T of a fetus at 23 + 4 GW: the corpus callosum (arrow) and the cerebral aqueduct (dashed arrow) can be delineated.

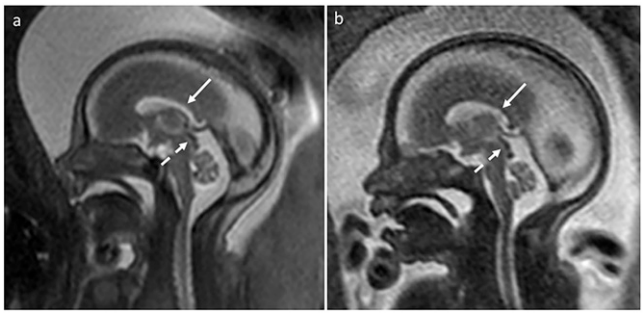

diffusion-weighted imaging), MR can discriminate even slight differences, depict small details, characterize the extent of damage and lead to a diagnosis. At 3.0 T, higher susceptibility allows depiction of deoxyhaemoglobin/haemosiderin on T2W images. EPI can depict intra-axial or extra-axial haemorrhage (Figure 4) and calcifications. In the near future, susceptibility-weighted imaging could become a useful imaging technique to delineate fine cerebral vascular structures[31] and delineate microhaemorrhages and calcifications.

Pathologies involving bones

A frequent question in fetal MR is whether there are facial defects.[32] In addition to the precise evaluation of the maxillo-facial anatomy and a demonstration of the extent of the defect (cleft lip, alveus, palate), associated anomalies can also be depicted. Besides T2W and SSFP sequences (Figure 5), EPI sequences (Figure 11) are best used to study the defects.[33] They should be acquired in the coronal, axial and sagittal planes. Higher susceptibility at 3.0 T facilitates delineation of ossified structures, counting vertebral bodies/rips. EPI sequence at 3.0 T better delineates subtle osseus structures of the fascia, for example the nasal bone (Figure 12), and evaluates, for *e.g.*, spinal

Figure 11. (a) Coronal echoplanar images at 3.0 T of a fetus at 26 + 5 GW and (b) at 1.5 T of a fetus at 29 + 3 GW.

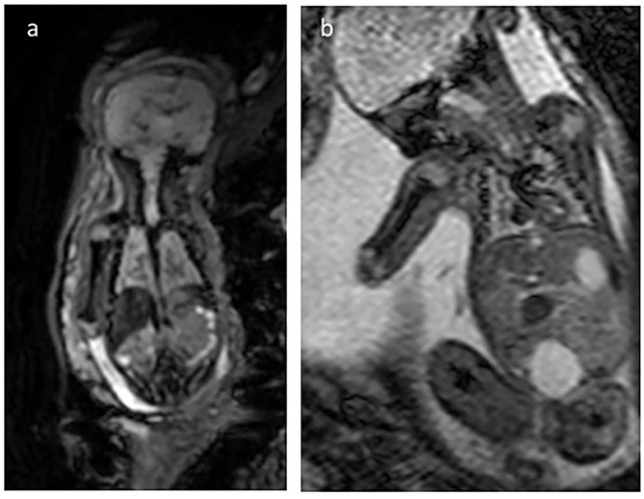

Figure 12. (a) Sagittal echoplanar images at 3.0 T of a fetus at 25 + 5 GW and (b) at 1.5 T of a fetus at 22 + 6 GW: the nasal bone (arrows) is clearly visible.

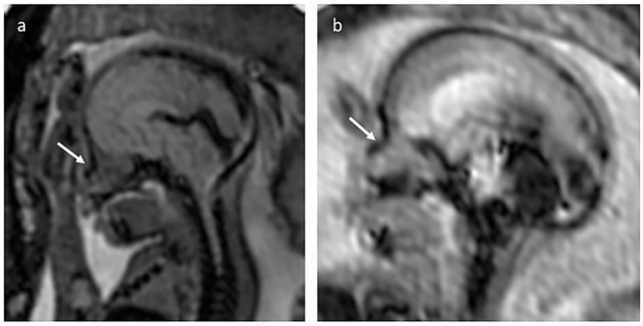

defects and skeletal dysplasias.[34] Higher susceptibility at 3.0 T also facilitates counting of vertebral bodies and ribs (Figure 5). In addition, the cartilage can be assessed with SSFP (Figure 5). In the future, susceptibility-weighted imaging might add useful information in this area. In addition, with thinner T1W images, the normal hyperintense-appearing fetal subcutaneous fat around the 27th gestational week (GW)[3] (Figure 13) and fatty replacement of affected muscles in the muscular dystrophies (Figure 14) can be evaluated.

Thoracoabdominal pathologies

In addition to the normal pulmonary tissue, which is subject to a substantial maturation process and can be followed with a change in T_1 and T_2 signal,[35] fetal MR can nicely delineate lung masses, which may be solid, cystic or mixed. The most common intrinsic lung lesions are congenital cystic adenomatoid malformations and pulmonary sequestration. Lung volumetry is an important prognostic parameter to assess pulmonary hypoplasia and may facilitate prenatal counselling and is achieved mainly with manual tracing on axial T2W slices over the thorax.[35–37] Here, with thinner T2W slices, the lung tissue can be traced

Figure 13. (a) Coronal T_1 weighted images of a fetus at 34 + 4 GW at 3.0 T and (b) at 34 + 5 GW at 1.5 T: the subcutaneous fat (arrows) is hyperintense.

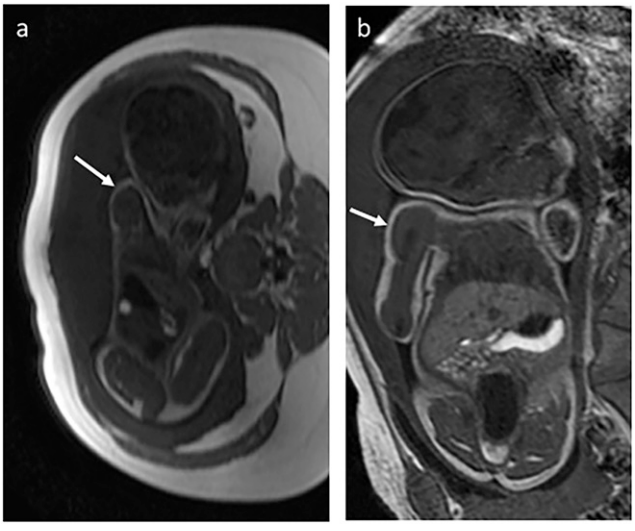

Figure 14. Series of sagittal T_2 weighted images at 3.0 T of a fetus at 22 + 2 GW with short and disfigured extremities: in the upper extremities, in particular, the dystrophic muscles can be seen (arrow).

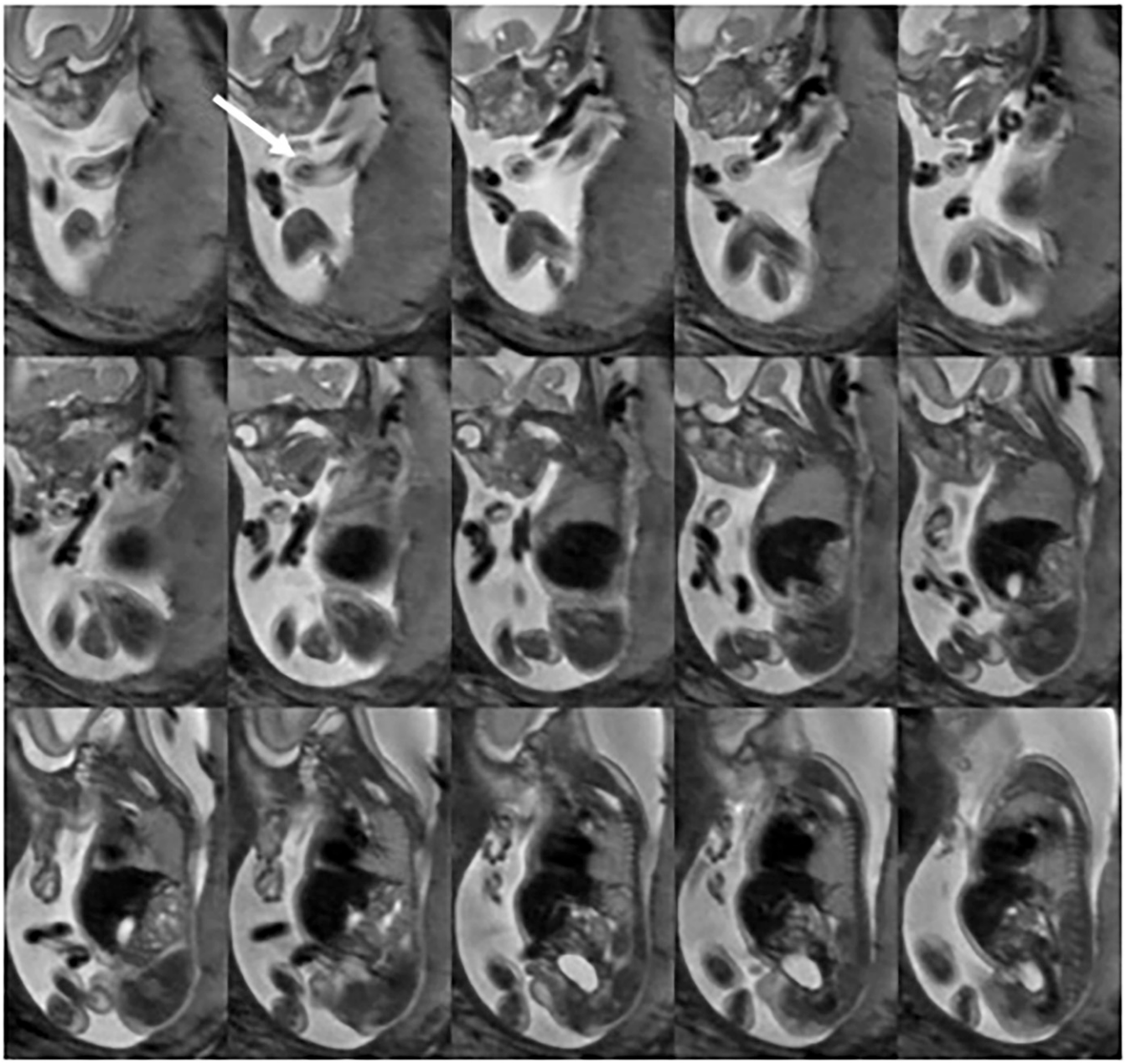

more exactly and the estimated lung volume will be more accurate. With thinner T2W slices, the feeding vessel in pulmonary sequestration can be visualized.

Congenital diaphragmatic hernia is an important fetal pathology, where abdominal contents enter the thoracic cavity through a defect in the diaphragm. The herniated organs compress the lungs and cause a mediastinal shift with deviation and compression of the heart. One important question in addition to the characterization of the herniated organs (Figure 15), assessment of the lung volume and pulmonary maturity is the measurement of the size and location of the defect,[38] where thinner slices might be helpful. In anterior wall defects, such as gastroschisis or in omphalocele, the assessment of the extent of herniation, content and width of the abdominal wall defect in gastroschisis is important.[39]

In the fetal gastrointestinal tract (GIT), one of the main uses of MRI is to assess the meconium, which is of hyperintense signal on T1W sequences (Figure 16) and is a sign of maturation of the GIT. Together with the fluid content in the rest of the bowel seen on a T2W sequence, bowel function and patency can be evaluated, for example, in GIT obstruction, such as oesophageal atresia, duodenal obstruction and small and large bowel stenosis. In atresia or stenosis, dilation of the bowel proximal to the site of obstruction can be depicted. A complication of intestinal atresia

Figure 15. (a) A coronal T_2 weighted (T2W) image at 3.0 T of a fetus at 32 + 6 GW with a left-sided congenital diaphragmatic hernia (CDH) and herniated bowel loops and stomach (arrow). (b) A coronal T2W image at 1.5 T of a fetus at 30 + 2 GW with a right-sided CDH and herniated liver (arrow).

may be perforation of the small bowel, which results in meconium peritonitis. At 3.0 T, thin T1W images (1.4 mm) show more details of meconium-filled bowel parts and might be helpful in evaluating complex malformations, such as cloacal dysgenesis, with a higher resolution and better contrast of the acquired images, position of the rectum in the pelvis and its position relative to the bladder. Organs such as the spleen, pancreas and uterus can be routinely delineated.[6]

Figure 16. (a) A coronal T_1 weighted (T1W) image of a fetus at 26 + 0 GW at 3.0 T. (b) A coronal T1W image at 1.5 T of a fetus at 26 + 3 GW. The meconium-stained bowel loops appear to be hyperintense (arrows).

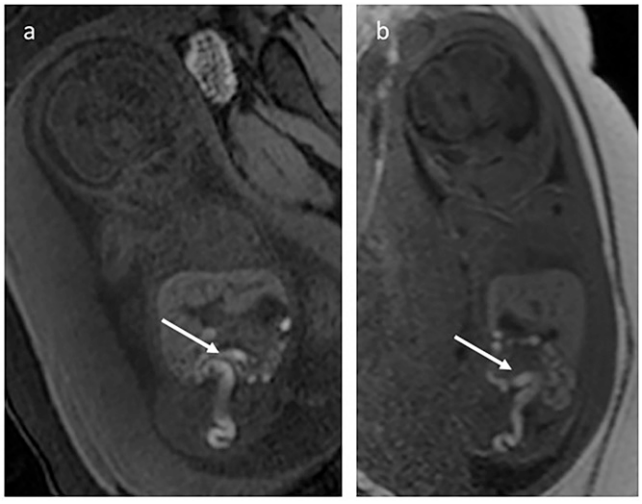

Figure 17. (a) Axial steady-state free-precession images at 3.0 T of the thorax with the heart of a fetus at 34 + 4 GW and (b) at 1.5 T of a fetus at 34 + 1 GW.

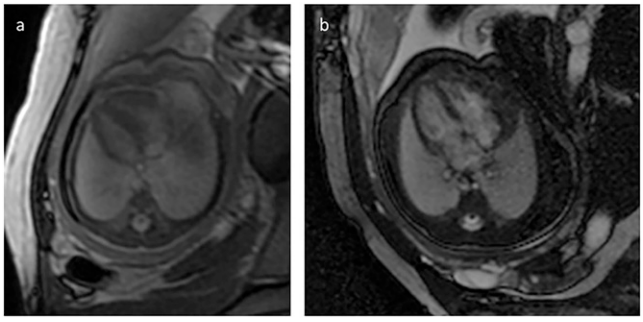

Vascular malformations

At 3.0 T, a higher sensitivity to flow leads to a better identification of vessels.[40]

Whether the higher field strength might have an impact on the characterization of other pathologies that have become routine indications for fetal MRI, such as pulmonary malformations,[35,41] placental imaging, heart imaging (Figure 17),[42] dynamic sequences for swallowing process, fetal general movements[43] or assessing residual kidney with diffusion-weighted imaging (Figure 18), has yet to be proved.

However, the use of 3.0 T also has some disadvantages compared with 1.5 T: most sequences have a longer duration (Table 1), making them more sensitive to motion-related artefacts and thus increasing the examination time, as more repetitions may be necessary than that at lower field strengths. In addition, artefacts from amniotic fluid cannot be completely avoided. As a consequence, pathologies associated with polyhydramnios,

Figure 18. (a) Coronal diffusion-weighted images at 3.0 T of a fetus at 26 + 5 GW and (b) at 1.5 T of a fetus at 33 + 6 GW: the typical hyperintense signal of the kidneys can be seen (arrows).

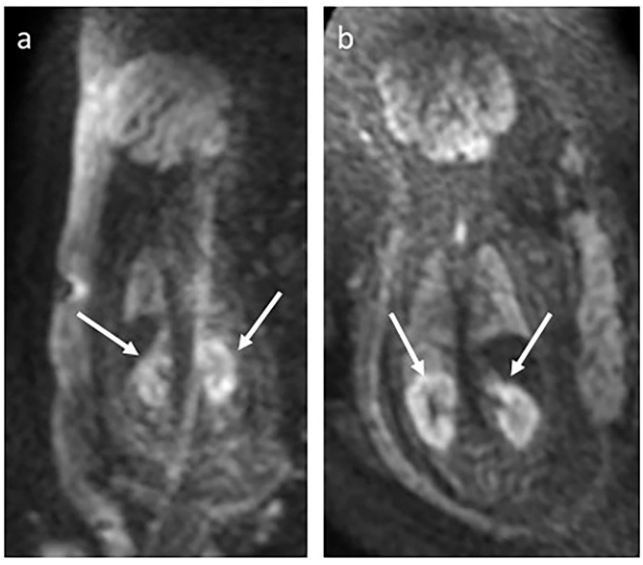

Table 1. Imaging parameters of sequences used in fetal MRI at 3.0 T (Achieva, Philips Medical Systems, Best, Netherlands). These are guidelines that must be adapted to the corresponding scanner

Sequence	FOV (mm)	Matrix	TR (ms)	TE (ms)	Flip angle (degree)	Slice thickness/ gap (mm)	Number of slices	Acquisition time (s)	Main indications
Survey T_1/TFE	450	256 × 128	8	2.3	15	5–8/0	31	41	Fetal position
Survey T_2/TSE	400	268 × 200	Shortest/3.5	Shortest/ 1.75	60	6/0	31	82	Fetal position
T_1 ultrafast GE FS	250	168 × 153	Shortest/ 3.12	1.49	10	1.5–3/0	31	21	Brain: haemorrhage, calcifications
T_1 ultrafast GE FS	375	252 × 230	Shortest/ 3.32	1.57	10	4/0	27–40	15–21	Body: thyroid, kidneys, digestive system (meconium)
T_1 ultrafast GE	250	168 × 153	Shortest/ 3.12	1.49	10	3/0	31	14	Haemorrhage, calcifications, fat
T_2 single-shot ultrafast SE	250	228 × 204	Shortest/ 5500–9800	200	90	2–3/0	25–32	25–35	Brain: anatomy, CSF
T_2 single shot ultrafast SE	280	256 × 229	Shortest/ 5400–8750	100	90	3–4/0	32–48	24–37	Body: lung development, stomach, airway
T_2 SSFP	250	168 × 125	Shortest/3.7	Shortest/ 1.83	90	6/−3	21	43	Brain: cysts
T_2 SSFP	400	268 × 200	Shortest/3.8	Shortest/ 1.90	90	4–6/0	21	38	Body: vessels, heart
FLAIR	230	112 × 89	7500	63.1	–	3.5/1	15–25	45	Brain: lamination, content of cystic lesions
GRE EPI	250	120 × 115	1000	35	90	2–3/0	23–31	8–16	Bone/cartilage, haemorrhage
DWI ($b = 700$)	400	132 × 134	4600	Shortest/ 65	90	5/0.5	84	78	Body: kidneys, haemorrhage
DWI ($b = 700$)	230	152 × 106	2247	Shortest/ 74	90	4/1.17	24	24	Brain: ischaemia, haemorrhage
SSFP Dynamic	450	212 × 281	2.8	1.39	90	10–30/2.35	120 (6 fps)	28	Fetal movements, swallowing
T_1 FFE dynamic	300	152 × 149	Shortest/3.1	Shortest/ 1.44	10	2	8 (6 fps)	37	Bowel movements
Single-shot MRCP	450	428 × 341	9449	487	90	40	9	106	3D fetus and surroundings
DTI (6 directions)	250	135 × 96	Shortest/ 1400	Shortest/ 112	90	4/0	15	106	Tractography
DTI (15 directions)	250	135 × 96	Shortest/856	Shortest/ 112	90	4/0	10	57	Tractography

(Continued)

Table 1. (Continued)

Sequence	FOV (mm)	Matrix	TR (ms)	TE (ms)	Flip angle (degree)	Slice thickness/ gap (mm)	Number of slices	Acquisition time (s)	Main indications
Spectroscopy	–	12 × 12	2000	144 or shorter	–	–	–	164	Metabolite measurement
BOLD	230	96 × 94	907	35	90	4	15	50	fMRI, placenta

3D, three-dimensional; BOLD, blood oxygen level dependent; CSF, cerebrospinal fluid; DTI, diffusion tensor imaging; DWI, diffusion-weighted imaging; EPI, echoplanar imaging; FFE, fast field echo; FLAIR, fluid-attenuated inversion recovery; fMRI, functional MRI; FOV, field of view; FS, fat saturated; GE, gradient echo; GRE, gradient recalled echo; MRCP, magnetic resonance cholangiopancreatography; SE, spin echo; SSFP, steady-state free-precession; TE, echo time; TFE, turbo field echo; TR, relaxation time; TSE, turbo spin echo.

such as oesophagus atresia, should rather be examined at lower field strengths. Tissue heating is also increased at 3.0 T,[44] albeit this heating is not dangerous for the fetus, it is uncomfortable for the pregnant female.

SAFETY CONCERNS

Of concern when scanning the fetus at a higher magnetic field strength is the energy absorbed by the fetus during MRI and measured in the form of specific absorption rate (SAR). Numerous studies conclude that there is no reason not to perform fetal MR on a 3.0 T system, although caution is suggested when performing scans without using a normal-level SAR mode, as the maximum local SAR value can be violated and may fall in the body of the fetus.[45,46] According to a recent study, the SAR of a fetal MR of the brain with adapted sequences is lower at 3.0 T than that at 1.5 T,[5] but contradictory to a previous publication.[47] Despite no evidence supporting any actual harm to the fetus, potentially unknown risks of SAR and RF energy deposition exist. Focal hot spots caused by RF field inhomogeneity and standing wave effects, where the SAR is higher, may complicate the effects of heating. Because of this, the SAR needs to be more closely monitored during 3.0 T examinations.

As a result, the Food and Drug Administration has imposed limits for RF exposure of 4 W kg^{-1} for maternal whole-body exposure, independent of the magnetic field strength, and scanner fail-safe mechanisms have been put in place to ensure these exposure levels are not exceeded. The International Commission on Non-Ionizing Radiation Protection (ICNIRP) 2004 guidelines state that the body temperature of the patient who is pregnant should not rise >0.5 °C and the temperature of the fetus should not exceed 38 °C.[48] With regard to the question of MR safe practices and the maximum field strength that can be applied, the report of the Canadian Task Force on Preventive Health Care concludes "Foetal magnetic resonance imaging is safe at 3.0 T or less during the second and third trimesters".[49] The practice parameter of the American College of Radiology concludes about fetal MR at 3.0 T: "At this stage, the preponderance of research studies have failed to discover any reproducible harmful effects of exposure of the mother or developing fetus to the 3.0 T or weaker magnetic fields used in the routine clinical MR imaging process. However, far less is known about the potential effects, if any, of the time varying gradient and/or RF magnetic fields used during actual scanning to potentiate image generation". And it goes on: "These theoretical risks should be carefully balanced against the potential benefits to the patient undergoing a MR examination".[50] More conservative in its conclusion is the British Association for Perinatal Medicine: "Given that doubling field strength increases the specific absorption rate (SAR) by a factor of 4, scanning at 3.0 T is currently not performed outside a research setting".[51] These findings suggest that care should be taken to monitor both the local and whole-body SAR in patients who are pregnant and suggest that if careful monitoring is performed, scanning of the fetus can be performed safely at both 1.5 and 3.0 T. In any case, all MRI equipment have a built-in system that prohibits exposure beyond the Food and Drug Administration limits (4.0 W kg^{-1}).

With regard to the potential risk of acoustic damage to the fetus at 3.0 T MRI, there are no data that there is a relevant effect on

Table 2. Indications and reasons for performing fetal MR at 3.0 or 1.5 T

Indications	Reasons
Indications for 3.0 T	
Brain	Intraparenchymal resolution
Bones	Sensitivity for susceptibility effects
Gestational age <GW 18	Resolution
Cartilage (joints)	Resolution
Abdominal organs (pancreas, uterus)	Resolution
Angiography	Background suppression
Indications for 1.5 T	
Polyhydramnios	Less sensitive to moving fluids
Maternal sensitivity to heat	Less warming
Multiplets	Shorter duration
Large maternal habitus	Less sensitive to artefacts

fetal audition. Gradient field switching produces acoustic noise, which may be detrimental to fetal auditory development.[52] Reports of evidence of hearing loss, shortened gestation and low birth weight in cases where the fetus was exposed to excessive noise *in utero* exist,[53] but this was caused by chronic maternal exposure to loud noise and not acute noise levels experienced during fetal MRI examinations. Despite the lack of evidence about the risk of acoustic damage to the fetus, some safety measures can be applied. For example, an acoustic foam, placed on the scanner table, can be used to further decrease sound transmission to the fetus. Recently, new advanced noise reduction technologies, referred to as "Quiet Suite" (Siemens) and "Silent Scan" (GE), were introduced, which act on fast gradient switches.

CONCLUSION

In general, with appropriate sequence adaptations, examinations of the fetus at 3.0 T are comparable with the images obtained at 1.5 T. Because of the higher image resolution and SNR, finer structures and lesions can be delineated at 3.0 T. A major drawback is that examinations at 3.0 T are more prone to artefacts, which complicates imaging the fetus for classic referrals (maternal obesity, polyhydramnios). It is important to decide which system might be better to address which indication (Table 2). But, is fetal MRI at 3.0 T ready for routine use? The final answer is, yes it is.

REFERENCES

1. Smith FW, Adam AH, Phillips WD. NMR imaging in pregnancy. *Lancet* 1983; **1**: 61–2. doi: https://doi.org/10.1016/S0140-6736(83)91588-X
2. Thomason ME, Dassanayake MT, Shen S, Katkuri Y, Alexis M, Anderson AL, et al. Cross-hemispheric functional connectivity in the human fetal brain. *Sci Transl Med* 2013; **5**: 173ra24. doi: https://doi.org/10.1126/scitranslmed.3004978
3. Victoria T, Jaramillo D, Roberts TP, Zarnow D, Johnson AM, Delgado J, et al. Fetal magnetic resonance imaging: jumping from 1.5 to 3 Tesla (preliminary experience). *Pediatr Radiol* 2014; **44**: 376–86; quiz 373–5. doi: https://doi.org/10.1007/s00247-013-2857-0
4. Gholipour A, Estroff JA, Barnewolt CE, Robertson RL, Grant PE, Gagoski B, et al. Fetal MRI: a technical update with educational aspirations. *Concepts Magn Reson Part A Bridg Educ Res* 2014; **43**: 237–66. doi: https://doi.org/10.1002/cmr.a.21321
5. Krishnamurthy U, Neelavalli J, Mody S, Yeo L, Jella PK, Saleem S, et al. MR imaging of the fetal brain at 1.5T and 3.0T field strengths: comparing specific absorption rate (SAR) and image quality. *J Perinat Med* 2015; **43**: 209–20. doi: https://doi.org/10.1515/jpm-2014-0268
6. Victoria T, Johnson AM, Edgar JC, Zarnow DM, Vossough A, Jaramillo D. Comparison between 1.5-T and 3-T MRI for fetal imaging: is there an advantage to imaging with a higher field strength? *AJR Am J Roentgenol* 2016; **206**: 195–201. doi: https://doi.org/10.2214/AJR.14.14205
7. Soher BJ, Dale BM, Merkle EM. A review of MR physics: 3T *versus* 1.5T. *Magn Reson Imaging Clin N Am* 2007; **15**: 277–90. doi: https://doi.org/10.1016/j.mric.2007.06.002
8. Ditchfield M. 3T MRI in paediatrics: challenges and clinical applications. *Eur J Radiol* 2008; **68**: 309–19. doi: https://doi.org/10.1016/j.ejrad.2008.05.019
9. Stanisz GJ, Odrobina EE, Pun J, Escaravage M, Graham SJ, Bronskill MJ, et al. T1, T2 relaxation and magnetization transfer in tissue at 3T. *Magn Reson Med* 2005; **54**: 507–12. doi: https://doi.org/10.1002/mrm.20605
10. Fillmer A, Kirchner T, Cameron D, Henning A. Constrained image-based B0 shimming accounting for "local minimum traps" in the optimization and field inhomogeneities outside the region of interest. *Magn Reson Med* 2015; **73**: 1370–80. doi: https://doi.org/10.1002/mrm.25248
11. Collins CM, Liu W, Schreiber W, Yang QX, Smith MB. Central brightening due to constructive interference with, without, and despite dielectric resonance. *J Magn Reson Imaging* 2005; **21**: 192–6. doi: https://doi.org/10.1002/jmri.20245
12. Prayer D. *Fetal MRI*. London, UK: Springer; 2011.
13. Merkle EM, Dale BM, Paulson EK. Abdominal MR imaging at 3T. *Magn Reson Imaging Clin N Am* 2006; **14**: 17–26. doi: https://doi.org/10.1016/j.mric.2005.12.001
14. Vernickel P, Roschmann P, Findeklee C, Ludeke KM, Leussler C, Overweg J, et al. Eight-channel transmit/receive body MRI coil at 3T. *Magn Reson Med* 2007; **58**: 381–9. doi: https://doi.org/10.1002/mrm.21294
15. Childs AS, Malik SJ, O'Regan DP, Hajnal JV. Impact of number of channels on RF shimming at 3T. *MAGMA* 2013; **26**: 401–10. doi: https://doi.org/10.1007/s10334-012-0360-5
16. Wieben O, Francois C, Reeder SB. Cardiac MRI of ischemic heart disease at 3 T: potential and challenges. *Eur J Radiol* 2008; **65**: 15–28. doi: https://doi.org/10.1016/j.ejrad.2007.10.022
17. Erturk SM, Alberich-Bayarri A, Herrmann KA, Marti-Bonmati L, Ros PR. Use of 3.0-T MR imaging for evaluation of the abdomen. *RadioGraphics* 2009; **29**: 1547–63. doi: https://doi.org/10.1148/rg.296095516
18. Levine D, Hulka CA, Ludmir J, Li W, Edelman RR. Placenta accreta: evaluation with color Doppler US, power Doppler US, and MR imaging. *Radiology* 1997; **205**: 773–6. doi: https://doi.org/10.1148/radiology.205.3.9393534
19. Rossi AC, Prefumo F. Additional value of fetal magnetic resonance imaging in the prenatal diagnosis of central nervous system anomalies:

a systematic review of the literature. *Ultrasound Obstet Gynecol* 2014; **44**: 388–93. doi: https://doi.org/10.1002/uog.13429
20. Weisz B, Hoffmann C, Ben-Baruch S, Yinon Y, Gindes L, Katorza E, et al. Early detection by diffusion-weighted sequence magnetic resonance imaging of severe brain lesions after fetoscopic laser coagulation for twin-twin transfusion syndrome. *Ultrasound Obstet Gynecol* 2014; **44**: 44–9. doi: https://doi.org/10.1002/uog.13283
21. Pugash D, Lehman AM, Langlois S. Prenatal ultrasound and MRI findings of temporal and occipital lobe dysplasia in a twin with achondroplasia. *Ultrasound Obstet Gynecol* 2014; **44**: 365–8. doi: https://doi.org/10.1002/uog.13359
22. Pugash D, Krssak M, Kulemann V, Prayer D. Magnetic resonance spectroscopy of the fetal brain. *Prenat Diagn* 2009; **29**: 434–41. doi: https://doi.org/10.1002/pd.2248
23. Charles-Edwards GD, Jan W, To M, Maxwell D, Keevil SF, Robinson R. Non-invasive detection and quantification of human foetal brain lactate in utero by magnetic resonance spectroscopy. *Prenat Diagn* 2010; **30**: 260–6. doi: https://doi.org/10.1002/pd.2463
24. Sanz-Cortes M, Simoes RV, Bargallo N, Masoller N, Figueras F, Gratacos E. Proton magnetic resonance spectroscopy assessment of fetal brain metabolism in late-onset "small for gestational age" *versus* "intrauterine growth restriction" fetuses. *Fetal Diagn Ther* 2015; **37**: 108–16. doi: https://doi.org/10.1159/000365102
25. Moore RJ, Strachan B, Tyler DJ, Baker PN, Gowland PA. *In vivo* diffusion measurements as an indication of fetal lung maturation using echo planar imaging at 0.5T. *Magn Reson Med* 2001; **45**: 247–53. doi: https://doi.org/10.1002/1522-2594(200102)45:2<247::AID-MRM1033>3.0.CO;2-M
26. Baldoli C, Righini A, Parazzini C, Scotti G, Triulzi F. Demonstration of acute ischemic lesions in the fetal brain by diffusion magnetic resonance imaging. *Ann Neurol* 2002; **52**: 243–6. doi: https://doi.org/10.1002/ana.10255
27. Bonel HM, Stolz B, Diedrichsen L, Frei K, Saar B, Tutschek B, et al. Diffusion-weighted MR imaging of the placenta in fetuses with placental insufficiency. *Radiology* 2010; **257**: 810–19. doi: https://doi.org/10.1148/radiol.10092283
28. Kostovic I, Judas M, Rados M, Hrabac P. Laminar organization of the human fetal cerebrum revealed by histochemical markers and magnetic resonance imaging. *Cereb Cortex* 2002; **12**: 536–44. doi: https://doi.org/10.1093/cercor/12.5.536
29. Kasprian G, Brugger PC, Weber M, Krssak M, Krampl E, Herold C, et al. In utero tractography of fetal white matter development. *Neuroimage* 2008; **43**: 213–24. doi: https://doi.org/10.1016/j.neuroimage.2008.07.026
30. Prayer D, Brugger PC, Kasprian G, Witzani L, Helmer H, Dietrich W, et al. MRI of fetal acquired brain lesions. *Eur J Radiol* 2006; **57**: 233–49. doi: https://doi.org/10.1016/j.ejrad.2005.11.023
31. Dai Y, Dong S, Zhu M, Wu D, Zhong Y. Visualizing cerebral veins in fetal brain using susceptibility-weighted MRI. *Clin Radiol* 2014; **69**: e392–7. doi: https://doi.org/10.1016/j.crad.2014.06.010
32. Mailath-Pokorny M, Worda C, Krampl-Bettelheim E, Watzinger F, Brugger PC, Prayer D. What does magnetic resonance imaging add to the prenatal ultrasound diagnosis of facial clefts? *Ultrasound Obstet Gynecol* 2010; **36**: 445–51.
33. Nemec U, Nemec SF, Weber M, Brugger PC, Kasprian G, Bettelheim D, et al. Human long bone development *in vivo*: analysis of the distal femoral epimetaphysis on MR images of fetuses. *Radiology* 2013; **267**: 570–80. doi: https://doi.org/10.1148/radiol.13112441
34. Nemec U, Nemec SF, Krakow D, Brugger PC, Malinger G, Graham JM Jr, et al. The skeleton and musculature on foetal MRI. *Insights Imaging* 2011; **2**: 309–18. doi: https://doi.org/10.1007/s13244-011-0075-6
35. Kasprian G, Balassy C, Brugger PC, Prayer D. MRI of normal and pathological fetal lung development. *Eur J Radiol* 2006; **57**: 261–70. doi: https://doi.org/10.1016/j.ejrad.2005.11.031
36. Zamora IJ, Sheikh F, Cassady CI, Olutoye OO, Mehollin-Ray AR, Ruano R, et al. Fetal MRI lung volumes are predictive of perinatal outcomes in fetuses with congenital lung masses. *J Pediatr Surg* 2014; **49**: 853–8; discussion 858. doi: https://doi.org/10.1016/j.jpedsurg.2014.01.012
37. Coleman A, Phithakwatchara N, Shaaban A, Keswani S, Kline-Fath B, Kingma P, et al. Fetal lung growth represented by longitudinal changes in MRI-derived fetal lung volume parameters predicts survival in isolated left-sided congenital diaphragmatic hernia. *Prenat Diagn* 2015; **35**: 160–6. doi: https://doi.org/10.1002/pd.4510
38. Mehollin-Ray AR, Cassady CI, Cass DL, Olutoye OO. Fetal MR imaging of congenital diaphragmatic hernia. *Radiographics* 2012; **32**: 1067–84. doi: https://doi.org/10.1148/rg.324115155
39. Brugger PC, Prayer D. Development of gastroschisis as seen by magnetic resonance imaging. *Ultrasound Obstet Gynecol* 2011; **37**: 463–70. doi: https://doi.org/10.1002/uog.8894
40. Tsai-Goodman B, Zhu MY, Al-Rujaib M, Seed M, Macgowan CK. Foetal blood flow measured using phase contrast cardiovascular magnetic resonance—preliminary data comparing 1.5 T with 3.0 T. *J Cardiovasc Magn Reson* 2015; **17**: 30. doi: https://doi.org/10.1186/s12968-015-0132-2
41. Di Prima FA, Bellia A, Inclimona G, Grasso F, Teresa M, Cassaro MN. Antenatally diagnosed congenital cystic adenomatoid malformations (CCAM): research review. *J Prenat Med* 2012; **6**: 22–30.
42. Saleem SN. Feasibility of MRI of the fetal heart with balanced steady-state free precession sequence along fetal body and cardiac planes. *AJR Am J Roentgenol* 2008; **191**: 1208–15. doi: https://doi.org/10.2214/AJR.07.3839
43. Nemec SF, Nemec U, Brugger PC, Bettelheim D, Rotmensch S, Graham JM Jr, et al. MR imaging of the fetal musculoskeletal system. *Prenat Diagn* 2012; **32**: 205–13. doi: https://doi.org/10.1002/pd.2914
44. Murbach M, Neufeld E, Samaras T, Corcoles J, Robb FJ, Kainz W, et al. Pregnant women models analyzed for RF exposure and temperature increase in 3T RF shimmed birdcages. *Magn Reson Med* 2016. [Epub ahead of print] doi: https://doi.org/10.1002/mrm.26268
45. Kanal E, Barkovich AJ, Bell C, Borgstede JP, Bradley WG Jr, Froelich JW, et al; Expert Panel on MR Safety. ACR guidance document on MR safe practices: 2013. *J Magn Reson Imaging* 2013; **37**: 501–30. doi: https://doi.org/10.1002/jmri.24011
46. Kikuchi S, Saito K, Takahashi M, Ito K. Temperature elevation in the fetus from electromagnetic exposure during magnetic resonance imaging. *Phys Med Biol* 2010; **55**: 2411–26. doi: https://doi.org/10.1088/0031-9155/55/8/018
47. Welsh RC, Nemec U, Thomason ME. Fetal magnetic resonance imaging at 3.0 T. *Top Magn Reson Imaging* 2011; **22**: 119–31. doi: https://doi.org/10.1097/RMR.0b013e318267f932
48. International Commission on Non-Ionizing Radiation Protection. Medical magnetic resonance (MR) procedures: protection of patients. *Health Phys* 2004; **87**: 197–216.
49. Patenaude Y, Pugash D, Lim K, Morin L, Bly S, Butt K, et al. The use of magnetic resonance imaging in the obstetric patient. *J Obstet Gynaecol Can* 2014; **36**: 349–63.
50. Radiology TACo. ACR–SPR practice parameter for the safe and optimal performance of fetal magnetic resonance imaging (MRI). 2015 (Resolution 11).
51. Medicine BAFP. Fetal and neonatal brain magnetic resonance imaging: clinical indications, acquisitions and reporting. [February 2016].
52. Bulas D, Egloff A. Benefits and risks of MRI in pregnancy. *Semin Perinatol* 2013; **37**: 301–4. doi: https://doi.org/10.1053/j.semperi.2013.06.005
53. Brezinka C, Lechner T, Stephan K. The fetus and noise. [In German.] *Gynakol Geburtshilfliche Rundsch* 1997; **37**: 119–29. doi: https://doi.org/10.1159/000272841